Circulation Journal
Official Journal of the Japanese Circulation Society
http://www.j-circ.or.jp

ORIGINAL ARTICLE
Arrhythmia/Electrophysiology

# Acceleration of $Ca^{2+}$ Waves in Monocrotaline-Induced Right Ventricular Hypertrophy in the Rat

Masahito Miura, MD, PhD; Masanori Hirose, MD, PhD; Hideaki Endoh, MD, PhD; Yuji Wakayama, MD, PhD; Yoshinao Sugai, MD, PhD; Makoto Nakano, MD, PhD; Koji Fukuda, MD, PhD; Chiyohiko Shindoh, MD, PhD; Kunio Shirato, MD, PhD; Hiroaki Shimokawa, MD, PhD

***Background:*** Triggered arrhythmias arise from delayed afterdepolarizations (DADs), with $Ca^{2+}$ waves playing an important role in their formation. In ventricular hypertrophy, however, it remains unclear how $Ca^{2+}$ waves change their propagation features and affect arrhythmogenesis. We addressed this important issue in a rat model of hypertrophy.

***Methods and Results:*** Rats were given a subcutaneous injection of 60 mg/kg monocrotaline (MCT-rats) or solvent (Ctr-rats). After 4 weeks, MCT-rats showed high right ventricular (RV) pressure and RV hypertrophy. Trabeculae were dissected from 36 right ventricles. The force was measured using a silicon strain gauge and regional intracellular $Ca^{2+}$ ($[Ca^{2+}]_i$) was determined using microinjected fura-2. Reproducible $Ca^{2+}$ waves were induced by stimulus trains (2 Hz, 7.5 s). MCT-rats showed a higher diastolic $[Ca^{2+}]_i$ and faster and larger $Ca^{2+}$ waves ($P<0.01$). The velocity and amplitude of $Ca^{2+}$ waves were correlated with the diastolic $[Ca^{2+}]_i$ both in the Ctr- and MCT-rats. The velocity of $Ca^{2+}$ waves in the MCT-rats was larger at the given amplitude of $Ca^{2+}$ waves than that in the Ctr-rats ($P<0.01$). The amplitude of DADs was correlated with the velocity and amplitude of $Ca^{2+}$ waves in the Ctr- and MCT-rats.

***Conclusions:*** The results suggest that an increase in diastolic $[Ca^{2+}]_i$ and an increase in $Ca^{2+}$ sensitivity of the sarcoplasmic reticulum $Ca^{2+}$ release channel accelerate $Ca^{2+}$ waves in ventricular hypertrophy, thereby causing arrhythmogenesis. (*Circ J* 2011; **75:** 1343–1349)

**Key Words:** $Ca^{2+}$ waves; Monocrotaline; Ventricular hypertrophy

Arrhythmias are likely to occur in diseased hearts,[1–3] and delayed afterdepolarizations (DADs) play an important role[4] in their occurrence, associated with catecholamine excess,[5] heart failure,[6] and mutations of the ryanodine receptor or calsequestrin.[7] Such diseased hearts not only exhibit an increase in diastolic intracellular $Ca^{2+}$ ($[Ca^{2+}]_i$),[8] which causes spontaneous $Ca^{2+}$ release from the sarcoplasmic reticulum (SR),[9,10] but also exhibit nonuniform muscle contraction,[11,12] which causes $Ca^{2+}$ dissociation from the myofilaments within the border zone between contracting and stretched regions during the relaxation phase.[10,13,14] Both the $Ca^{2+}$ released from the SR and that dissociated from the myofilaments can induce $Ca^{2+}$ waves, which propagate along the myocardium by the mechanism of $Ca^{2+}$-induced $Ca^{2+}$ release from the SR.[15] Since the velocity and amplitude of $Ca^{2+}$ waves determine the formation of DADs[16] (ie, arrhythmogenesis principally through the activation of the $Na^+$–$Ca^{2+}$ exchange (NCX) current[16,17]), it is still important to investigate the propagation features of the $Ca^{2+}$ waves.

It has been reported that in ventricular hypertrophy, 6 clear changes occur with maladaptive remodeling of the myocardium: (1) reduction of SR $Ca^{2+}$ ATPase (SERCA2a),[18] (2) increase in level of NCX,[19] (3) prolonged action potentials,[20] (4) altered transverse tubules, (5) development of dyssynchronous $Ca^{2+}$ release, and (6) increased SR $Ca^{2+}$ leakage.[21] Of these 6, reports about SR $Ca^{2+}$ leakage have been inconsistent as to the amplitude and frequency of $Ca^{2+}$ sparks in ventricular hypertrophy.[22–24] Additionally, it has even been reported that $Ca^{2+}$ waves caused by $Ca^{2+}$ sparks propagate more slowly in ventricular hypertrophy.[22] Furthermore, it

Received October 13, 2010; revised manuscript received January 11, 2011; accepted February 16, 2011; released online April 2, 2011 Time for primary review: 20 days

Department of Clinical Physiology, Health Science (M.M., C.S.), Department of Cardiovascular Medicine (M.H., H.E., Y.W., Y.S., M.N., K.F., K.S., H.S.), Tohoku University Graduate School of Medicine, Sendai, Japan

The first two authors contributed equally to this work (M.M., M.H.).

The Guest Editor for this article was Tetsunori Saikawa, MD.

Mailing address: Masahito Miura, MD, PhD, Department of Clinical Physiology, Health Science, Tohoku University Graduate School of Medicine, 2-1 Seiryo-machi, Aoba-ku, Sendai 980-8574, Japan. E-mail: mmiura@med.tohoku.ac.jp

ISSN-1346-9843 doi:10.1253/circj.CJ-10-1050

**Table 1. General and Cardiac Characteristics of Ctr and MCT-Exposed Rats**

| | Ctr-rats (n=9–18) | MCT-rats (n=9–18) |
|---|---|---|
| HR, beats/min | 356±10 | 340±13 |
| mRAP, mmHg | 2.65±0.23 | 4.39±0.34** |
| sRVP, mmHg | 20.5±1.1 | 47.3±7.8** |
| Body weight, g | 350±6 | 331±9 |
| Heart weight, g | 0.93±0.01 | 1.08±0.03** |
| RV weight, g | 0.20±0.01 | 0.36±0.02** |
| RV weight/body weight, mg/g | 0.57±0.03 | 1.10±0.04** |
| RV/(LV+IVS) weight | 0.27±0.01 | 0.51±0.02** |
| Lung weight, g | 1.39±0.03 | 2.03±0.06** |
| Liver weight, g | 13.9±0.4 | 13.1±0.5 |

Results are mean±SEM. **P<0.01 vs. Ctr-rats.
Ctr, control; MCT, monocrotaline; HR, heart rate; mRAP, mean right atrial pressure; sRVP, systolic right ventricular pressure; RV, right ventricle; LV, left ventricle; IVS, interventricular septum.

remains unclear how the propagation features of $Ca^{2+}$ waves, especially those induced by $Ca^{2+}$ dissociated from the myofilaments, are changed and affect arrhythmogenesis in ventricular hypertrophy.

Thus, in the present study, we observed the propagation features of $Ca^{2+}$ waves, principally those induced by $Ca^{2+}$ dissociated from the myofilaments, in the trabeculae obtained from a rat model of monocrotaline (MCT)-induced pulmonary hypertension and right-sided ventricular hypertrophy.

## Methods

### Animal Model

All animal procedures were performed according to the *Guide for the Care and Use of Laboratory Animals* published by the US National Institutes of Health (NIH Publication No. 85–23, revised 1996) and were approved by the Ethics Review Board of Tohoku University (approval reference no. 21–98). Sprague-Dawley rats weighing 200 g received a single subcutaneous injection of 60 mg/kg MCT (MCT-rats) or an equal volume of solvent (Ctr-rats), as previously described.[25] Four weeks after the injection, 25.4% of the MCT-rats died from right-sided heart failure but none of the Ctr-rats died. The

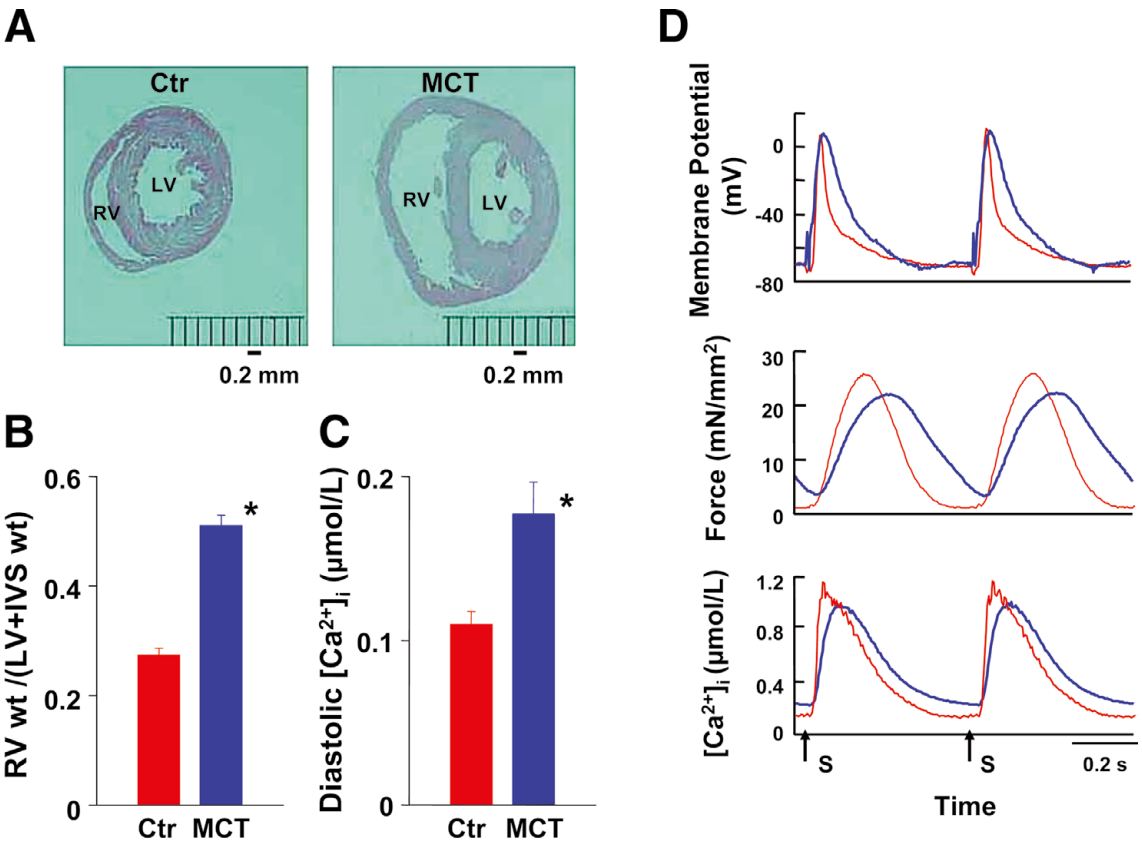


**Figure 1.** Characteristics of monocrotaline (MCT)-induced right ventricular hypertrophy. (**A**) Representative section along the short axis of a heart from control (Ctr) and MCT-exposed rats (28 days). Note that the right ventricle (RV) is thickened and elongated and that its cavity is enlarged in the MCT-rat. (**B**,**C**) RV-to-(LV+IVS) weight ratio (**B**) and diastolic intracellular $Ca^{2+}$ (**C**) of Ctr- and MCT-rats. They were significantly larger in the MCT-rats. LV, left ventricle; IVS, intraventricular septum. *P<0.01 vs. Ctr-rats. (**D**) Representative recordings of action potential (**Top**), developed force (**Middle**) and $Ca^{2+}$ transient (**Bottom**) in the Ctr- (red lines, 21.8°C, experiment no. 030114) and MCT-rats (blue lines, 22.0°C, experiment no. 021224) at 2 Hz stimulation ($[Ca^{2+}]_o$=2.0 mmol/L). Arrows with S indicate the moments of electrical stimulation.

survivors were anesthetized, the right atrial and ventricular pressures were measured, and then the heart was excised for sample preparation and heart weight measurement.

### Measurements of Force, $[Ca^{2+}]_i$, and Membrane Potential

Trabeculae were obtained as previously described (see online Supplemental File).[13–16] Briefly, trabeculae (n=36; length: 2.2±0.1 mm, width: 284±79 $\mu$m, thickness: 99±5 $\mu$m in slack condition) were dissected from the right ventricle (RV) of rats and mounted between a force transducer and a micromanipulator in a bath perfused by HEPES solution on an inverted microscope. Membrane potential was measured using ultra-compliant glass microelectrodes and sarcomere length (SL) was measured using laser diffraction techniques, as previously described.[13]

$[Ca^{2+}]_i$ was measured as previously described.[13,15] Briefly, fura-2 pentapotassium salt was microinjected electrophoretically into each trabecula. Excitation light of 340, 360, or 380 nm was used and fluorescence was collected using an image-intensified CCD camera at 30 frames/s to assess local $[Ca^{2+}]_i$. We calculated $[Ca^{2+}]_i$ in a region of interest along the trabeculae from the calibrated ratio of $F_{360}/F_{380}$[13–15] and constructed the 3-dimensional image. The velocity of the $Ca^{2+}$ wave was calculated from the slope of the fitted line to the plot between the time and the position of the peak point of the $Ca^{2+}$ transient during the $Ca^{2+}$ wave at each pixel along the trabecula (see online **Supplemental Data S1**).

**Table 2. Membrane Potential, Developed Force, and $Ca^{2+}$ Transient at 2 Hz Electrical Stimulation in Ctr and MCT-Exposed Rats**

| | Ctr-rats (n=5–7) | MCT-rats (n=7–9) |
|---|---|---|
| $APD_{90}$, ms | 205±11 | 320±20** |
| Force, mN/mm$^2$ | 29.4±2.7 | 21.5±1.8* |
| Peak $[Ca^{2+}]_i$, nmol/L | 1,027±33 | 819±30** |
| Diastolic $[Ca^{2+}]_i$, nmol/L | 110±8 | 177±20** |
| $\Delta[Ca^{2+}]_T$, nmol/L | 896±33 | 606±37** |
| $[Ca^{2+}]_i$ decline, ms | 106±15 | 167±18* |

Results are mean±SEM. Ctr-rats, 21.9±0.1°C; MCT-rats, 22.0±0.1°C; $[Ca^{2+}]_o$=2.0 mmol/L. *P<0.05, **P<0.01 vs. Ctr-rats. $APD_{90}$, action potential duration at 90% repolarization; $[Ca^{2+}]_i$, intracellular $Ca^{2+}$ concentration; $\Delta[Ca^{2+}]_T$, amplitude of $Ca^{2+}$ transient induced by electrical stimulation. Other abbreviations see in Table 1.

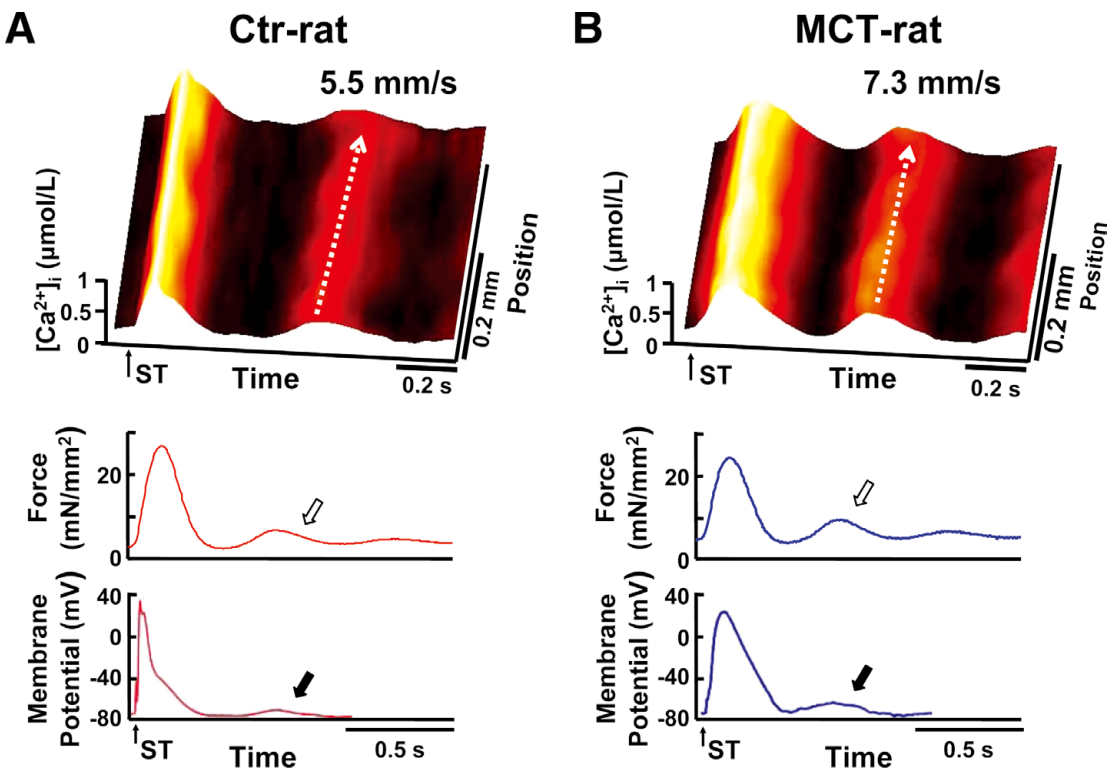


**Figure 2.** Regional changes in intracellular $Ca^{2+}$ ($[Ca^{2+}]_i$), force, and membrane potential in a control (Ctr)-rat and a monocrotaline (MCT)-exposed rat. (**Top**) Regional $[Ca^{2+}]_i$ calculated from the CCD camera images during the last electrically stimulated twitch of a train and the following aftercontraction. In these 3-D representations, the abscissa is time, the ordinate is $[Ca^{2+}]_i$, and the Z axis is the position along the long axis of the trabecula. After the end of the clearly uniform $Ca^{2+}$ transient by the last stimulus of a train (arrow with ST), a small $Ca^{2+}$ transient appeared to move like a wave from the one end (dotted arrow). Corresponding changes in force and membrane potential (**Middle** and **Bottom**). After the last electrically stimulated twitch of a train, aftercontractions (open arrows in middle panels) and delayed afterdepolarizations (closed arrows in bottom panels) occurred spontaneously ($[Ca^{2+}]_o$=3.0 mmol/L). (**A**) In a Ctr-rat, the calculated velocity of the $Ca^{2+}$ wave was 5.5 mm/s and the amplitude of the aftercontraction was 4.3 mN/mm$^2$ (22.1°C, experiment no. 021021). (**B**) In a MCT-exposed rat, the calculated velocity of the $Ca^{2+}$ wave was 7.3 mm/s and the amplitude of the aftercontraction was 6.7 mN/mm$^2$ (22.0°C, experiment no. 021114).

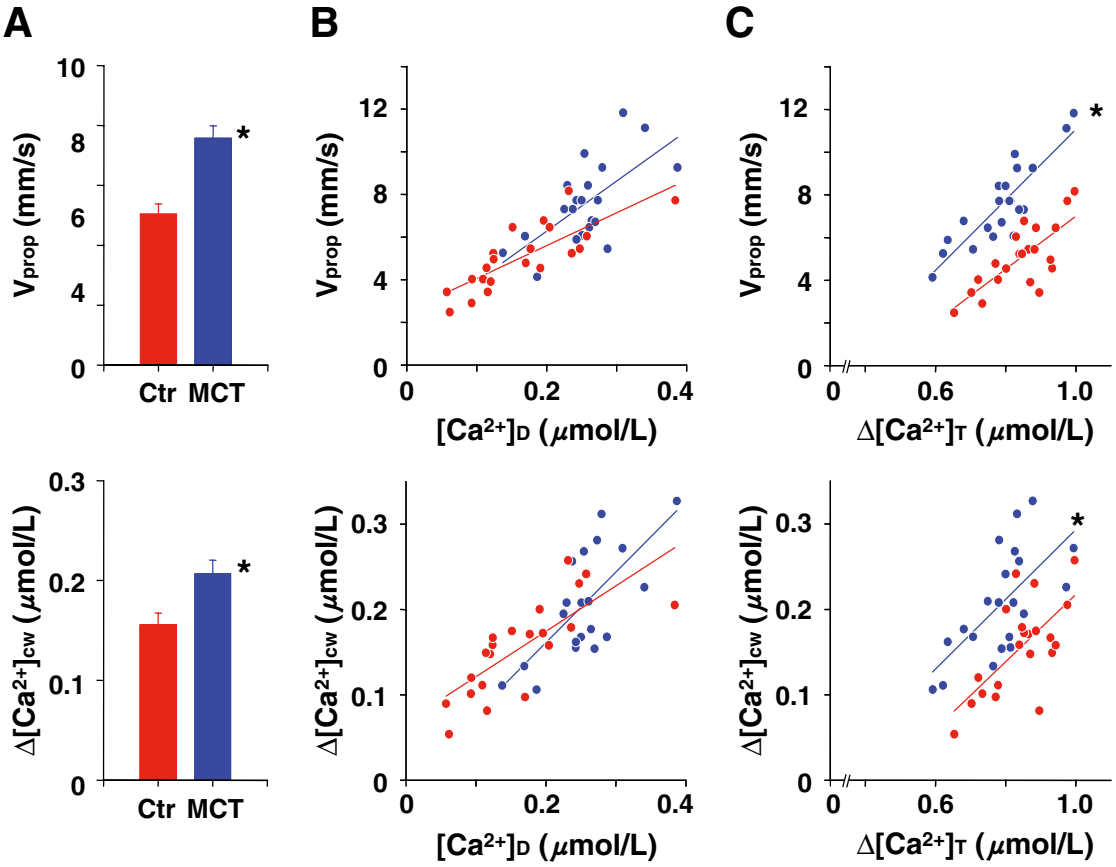


**Figure 3.** Changes in the velocity ($V_{prop}$) and amplitude ($\Delta[Ca^{2+}]_{CW}$) of $Ca^{2+}$ waves depending on the diastolic $[Ca^{2+}]_i$ ($[Ca^{2+}]_D$) and the amplitude of $Ca^{2+}$ transients by electrical stimulation ($\Delta[Ca^{2+}]_T$) in control rats (Ctr-rats, n=21, red bar or circles) and in monocrotaline-exposed rats (MCT-rats, n=21, blue bar or circles). Temperature was 22.1±0.3°C. (**A**) The $V_{prop}$ and $\Delta[Ca^{2+}]_{CW}$ of $Ca^{2+}$ waves are significantly larger in the MCT-rats, regardless of the $[Ca^{2+}]_o$ being lower in MCT-rats (Ctr-rats, $[Ca^{2+}]_o$=3.8±0.3 mmol/L; MCT-rats, $[Ca^{2+}]_o$=3.2±0.3 mmol/L). *P<0.01 vs. Ctr-rats. (**B**) Relationships of the $V_{prop}$ and $\Delta[Ca^{2+}]_{CW}$ of $Ca^{2+}$ waves against the $[Ca^{2+}]_D$. In the upper panel, the $V_{prop}$ linearly correlates with the $[Ca^{2+}]_D$ in the Ctr- (r=0.80) and MCT-rats (r=0.65). In the lower panel, the $\Delta[Ca^{2+}]_{CW}$ linearly correlates with the $[Ca^{2+}]_D$ in the Ctr- (r=0.76) and MCT-rats (r=0.71). In both panels, ANOCOVA analysis shows that the plots in Ctr- and MCT-rats are parallel and not significantly different. (**C**) Relationships of the $V_{prop}$ and $\Delta[Ca^{2+}]_{CW}$ of $Ca^{2+}$ waves against the $\Delta[Ca^{2+}]_T$. In the upper panel, the $V_{prop}$ linearly correlates with the $\Delta[Ca^{2+}]$ in the Ctr- (r=0.75) and MCT-rats (r=0.87). ANOCOVA analysis shows that the plots in Ctr- and MCT-rats are parallel and that the plots in MCT-rats are shifted upward. In the lower panel, the $\Delta[Ca^{2+}]_{CW}$ linearly correlates with the $\Delta[Ca^{2+}]_T$ in the Ctr- (r=0.66) and MCT-rats (r=0.66). ANOCOVA analysis shows that the plots in Ctr- and MCT-rats are parallel and that the plots in MCT-rats are shifted upward. *P<0.01 vs. Ctr-rats.

### Experimental Protocol

We first measured action potentials, developed force, and $Ca^{2+}$ transients at 2.0 Hz electrical stimulation in trabeculae from 7 Ctr-rats and 7 MCT-rats ($[Ca^{2+}]_o$=2.0 mmol/L, temperature=21.9±0.1°C). To induce $Ca^{2+}$ waves, trains of electrical stimuli at 2 Hz were then applied for 7.5 s ($[Ca^{2+}]_o$=2 mmol/L). After the measurement of the force and $Ca^{2+}$ waves, $[Ca^{2+}]_o$ was increased in steps of 0.5 mmol/L to remeasure the force and $Ca^{2+}$ waves by raising $Ca^{2+}$ levels within the muscle. In the present study, we analyzed the $Ca^{2+}$ waves arising from the end regions of the trabeculae since it has been reported that $Ca^{2+}$ dissociated from the myofilaments plays an important role in their initiation.[10,13–15] Eventually, 21 $Ca^{2+}$ waves in trabeculae from 7 Ctr-rats ($[Ca^{2+}]_o$=3.8±0.3 mmol/L) and 21 $Ca^{2+}$ waves in trabeculae from 6 MCT-rats ($[Ca^{2+}]_o$=3.2±0.3 mmol/L) were analyzed (temperature=22.1±0.3°C). The membrane potential during 13 $Ca^{2+}$ waves in trabeculae from 6 Ctr-rats and 7 $Ca^{2+}$ waves in trabeculae from 3 MCT-rats was also measured ($[Ca^{2+}]_o$=3.0±0.3 mmol/L). All measurements were performed at the SL of 2.1 μm.

### Statistical Analysis

All measurements are expressed as mean±SEM. Statistical analysis was performed with an unpaired Student's t-test for 2-group comparisons and analysis of covariance (ANOCOVA) for the other comparisons. Values of P<0.05 were considered significant.

## Results

In the MCT-rats, RV systolic pressure was higher and the wet tissue weight of the RV free wall was heavier than those in the Ctr-rats (**Table 1**, **Figures 1A**,**B**), suggesting that RV hypertrophy in the present study was induced by pulmonary

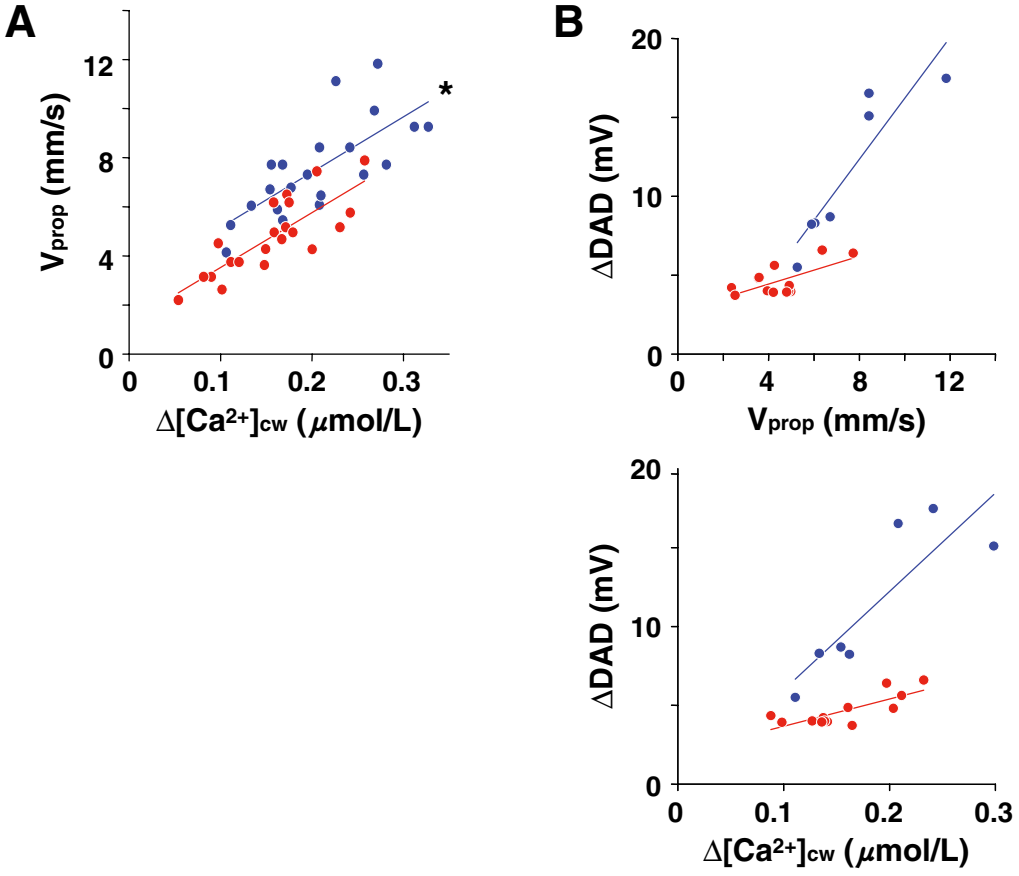


**Figure 4.** Effect of the velocity ($V_{prop}$) and ampltude ($\Delta[Ca^{2+}]_{CW}$) of $Ca^{2+}$ waves on the amplitude of delayed afterdepolarization (ΔDAD) in control rats (Ctr-rats, red circles) and in monocrotaline-exposed rats (MCT-rats, blue circles). (**A**) Relationships between the $V_{prop}$ of $Ca^{2+}$ waves and the $\Delta[Ca^{2+}]_{CW}$ of those in the Ctr- (r=0.81, n=21) and MCT-rats (r=0.73, n=21). ANOCOVA analysis shows that the plots in Ctr- and MCT-rats are parallel and that the plots in MCT-rats are shifted upward (*P<0.01 vs. Ctr-rats). (**B**) Relationships of the ΔDAD against the $V_{prop}$ and $\Delta[Ca^{2+}]_{CW}$ of $Ca^{2+}$ waves in the Ctr- (n=13, $[Ca^{2+}]_o$=2.9±0.4) and MCT-rats (n=7, $[Ca^{2+}]_o$=3.0±0.4). The ΔDAD linearly correlates with the $V_{prop}$ in the Ctr- (r=0.66) and MCT-rats (r=0.91) and linearly correlates with $\Delta[Ca^{2+}]_{CW}$ in the Ctr- (r=0.78) and MCT-rats (r=0.86). ANOCOVA analysis shows that the plots in Ctr- and MCT-rats are not parallel. Temperature was 22.0±0.2°C.

hypertension in the MCT-rats. The contractile properties of the Ctr- and MCT-rats at 2 Hz electrical stimulation are shown in **Table 2** and **Figures 1C,D**. In the MCT-rats, the time to 90% repolarization of the action potential was longer, the amplitude of the developed force was lower, and the $Ca^{2+}$ transients declined more slowly after reaching the lower peak values. The diastolic $[Ca^{2+}]_i$ was higher in MCT-rats.

**Figure 2** shows representative changes in the regional $[Ca^{2+}]_i$, force development, and membrane potential during the last electrically stimulated twitch of a train and the changes after the cessation of the train. The electrical stimulation induced a $Ca^{2+}$ wave arising from one end of each trabecula both in the Ctr- and MCT-rats. Importantly, the $Ca^{2+}$ wave induced in the MCT-rat was faster than that in the Ctr-rat, although each wave was induced under the same conditions. The summary data in **Figure 3A** show that the velocity and amplitude of $Ca^{2+}$ waves in the MCT-rats were significantly larger than those in the Ctr-rats, regardless of $[Ca^{2+}]_o$ at the measurements being lower in MCT-rats. Besides, in both the Ctr- and MCT-rats, the velocity and amplitude of $Ca^{2+}$ waves linearly correlated with the diastolic $[Ca^{2+}]_i$ (**Figure 3B**). Note that the relationships of the velocity and amplitude of $Ca^{2+}$ waves against the diastolic $[Ca^{2+}]_i$ in the MCT-rats were not discriminated from those in Ctr-rats, suggesting that the increases in both the velocity and the amplitude of $Ca^{2+}$ waves in MCT-rats, shown in **Figure 3A**, were merely caused by the increase in diastolic $[Ca^{2+}]_i$.

To investigate the effect of releasable $Ca^{2+}$ in the SR on the propagation features of $Ca^{2+}$ waves, we plotted the velocity and amplitude of $Ca^{2+}$ waves against the amplitude of $Ca^{2+}$ transients by electrical stimulation in both the Ctr- and MCT-rats (**Figure 3C**). In both groups of rats, the velocity and amplitude of $Ca^{2+}$ waves linearly correlated with the amplitude of $Ca^{2+}$ transients by electrical stimulation. Importantly, their relationships in MCT-rats significantly shifted upward compared with those in Ctr-rats, showing that $Ca^{2+}$ waves become faster and larger in MCT-rats despite containing the identical amount of releasable $Ca^{2+}$ within the SR.

It is well known that $Ca^{2+}$ waves propagate along the myocardium by the mechanism of $Ca^{2+}$-induced $Ca^{2+}$ release from the SR.[10] This means that when more $Ca^{2+}$ is released from the SR during $Ca^{2+}$ wave propagation, the propagation veloc-

ity becomes faster, because in this case the $[Ca^{2+}]_i$ level more rapidly reaches the threshold of $Ca^{2+}$ release in the neighboring SR. Actually, the propagation velocity of $Ca^{2+}$ waves linearly correlated with the amplitude of $Ca^{2+}$ waves in both the MCT-rats and Ctr-rats, as shown in **Figure 4A**. Interestingly, their relationship in MCT-rats significantly shifted upward compared with that in Ctr-rats, showing that $Ca^{2+}$ can induce $Ca^{2+}$ release from neighboring SR with a lower threshold in MCT-rats. Furthermore, the amplitude of DADs correlated with the velocity and amplitude of $Ca^{2+}$ waves (**Figure 4B**), suggesting that acceleration of $Ca^{2+}$ waves can enhance arrhythmogenesis in both Ctr- and MCT-rats.

## Discussion

In the present study, the propagation features of $Ca^{2+}$ waves in ventricular hypertrophy were characterized by directly measuring the spatial and temporal changes in $[Ca^{2+}]_i$ using multicellular ventricular muscle obtained from a rat model of MCT-induced pulmonary hypertension and RV hypertrophy. To the best of our knowledge, the present study shows for the first time that an increase in diastolic $[Ca^{2+}]_i$ and an increase in the $Ca^{2+}$ sensitivity of the SR $Ca^{2+}$ release channel accelerate $Ca^{2+}$ waves in ventricular hypertrophy, thereby causing arrhythmogenesis, as discussed next.

### MCT-Induced RV Hypertrophy

As in our previous studies,[25] we used MCT-rats as an experimental model of pulmonary hypertension-induced RV hypertrophy. MCT is a pyrrolizidine alkaloid, and its bioactive metabolite selectively injures the vascular endothelium of lung vessels. Progressive pulmonary vasculitis leads to increasing vascular resistance and a gradual rise in arterial pressure starting ~14 days after a single dose of MCT.[26] The increase in RV afterload induces hypertrophy, which progresses to dilation and failure.[26] Also in the present study, the MCT-rats showed higher systolic RV pressure, RV hypertrophy, and an increase in diastolic $[Ca^{2+}]_i$ (**Tables 1**,**2**, **Figure 1**). In addition, our previous report showed that MCT-rats exhibit a lower expression of SERCA2 protein and a relatively higher expression of NCX protein.[25] These properties of MCT-rats are consistent with past reports for the same experimental model[27,28] and for other animal models of ventricular hypertrophy.[29] Thus, we are convinced that MCT-rats can serve as a model of ventricular hypertrophy to examine the propagation features of $Ca^{2+}$ waves.

### Acceleration of $Ca^{2+}$ Waves

Since both the ends of the trabeculae are fixed in this experimental setup,[13–15] the end regions are stretched during muscle contraction and are shortened during muscle relaxation. By the shortening of the muscle during relaxation, $Ca^{2+}$ is dissociated from the myofilaments within the end regions[14] due to the altered affinity of the myofilaments for $Ca^{2+}$.[30] We consider that this $Ca^{2+}$ dissociated from the myofilaments within the end regions induces the $Ca^{2+}$ waves arising from the end regions of trabeculae, as observed in the present study.[14] The observation that these waves disappear at low afterload by reducing muscle length[31] supports this idea. For this reason, it is not appropriate to compare the $Ca^{2+}$ waves in the present study with those observed under conditions of slack length in isolated myocytes.[22]

The increase in diastolic $[Ca^{2+}]_i$ in the MCT-rats (**Table 2**, **Figures 1C**,**D**) may be caused by the lower expression of SERCA protein[25] because it has been reported that diastolic $[Ca^{2+}]_i$ inversely correlates with SERCA activity.[32] This increase in diastolic $[Ca^{2+}]_i$ can increase $Ca^{2+}$ release from the SR due to activation of the SR $Ca^{2+}$ release channel[33] and facilitate the diffusion of $Ca^{2+}$ ions,[15] thereby causing the acceleration of $Ca^{2+}$ waves in the MCT-rats (**Figures 2**,**3A**, **B**).

The upward shift in the relationships in the MCT-rats shown in **Figure 3C** means that, in the MCT-rats, the $[Ca^{2+}]_i$ level more rapidly reaches the threshold of $Ca^{2+}$ release from neighboring SR and releases more $Ca^{2+}$ despite containing the identical amount of releasable $Ca^{2+}$ within the SR during $Ca^{2+}$ wave propagation, suggesting that $Ca^{2+}$ sensitivity of the SR $Ca^{2+}$ release channel is increased in MCT-rats.[34] Besides, the upward shift in the relationship between the velocity of $Ca^{2+}$ waves and the amplitude of those in the MCT-rats, shown in **Figure 4A**, means that in the MCT-rat, the $[Ca^{2+}]_i$ level more rapidly reaches the threshold of $Ca^{2+}$ release from neighboring SR when the identical amount of $Ca^{2+}$ is released from the SR during $Ca^{2+}$ wave propagation, again suggesting that the $Ca^{2+}$ sensitivity of the SR $Ca^{2+}$ release channel is increased in MCT-rats. This upward shift in their relationship has also been observed after the addition of 0.1 or 0.3 mmol/L caffeine.[15] Since low concentrations of caffeine have been reported to accelerate $Ca^{2+}$ waves[15] by increasing $Ca^{2+}$ sensitivity of the SR $Ca^{2+}$ release channel[35] or by directly increasing the probability of its opening,[36] it is probable that in ventricular hypertrophy, $Ca^{2+}$ waves are accelerated by the same mechanism as for caffeine. Actually, it has been reported that in failing hearts, the SR $Ca^{2+}$ release channel is phosphorylated[37] and exhibits a higher $Ca^{2+}$ sensitivity,[38] suggesting that in ventricular hypertrophy, this higher $Ca^{2+}$ sensitivity of the SR $Ca^{2+}$ release channel may also be involved in the acceleration of $Ca^{2+}$ waves.

The amplitude of DADs linearly correlated with the velocity and amplitude of $Ca^{2+}$ waves, probably through the NCX current (**Figure 4**),[16,17] suggesting that, in the present study, acceleration of $Ca^{2+}$ waves enhanced arrhythmogenesis in both the Ctr- and MCT-rats. The steeper slope of the relationship in the MCT-rats may be due to the increased expression of the NCX.[19,25]

In conclusion, the results of the present study suggest that an increase in diastolic $[Ca^{2+}]_i$ and an increase in the $Ca^{2+}$ sensitivity of the SR $Ca^{2+}$ release channel accelerate $Ca^{2+}$ waves in ventricular hypertrophy, thereby causing arrhythmogenesis.

### Study Limitations

We did not measure $[Ca^{2+}]_i$ changes at the subcellular level because muscle contractions are essential for the induction of $Ca^{2+}$ waves arising from the end regions of the trabeculae[31] and the movement of trabeculae during muscle contractions makes measurement using confocal microscopy difficult. For this reason, we did not observe whether $Ca^{2+}$ ions really dissociate from the myofilaments[30] and initiate $Ca^{2+}$ waves within the end regions of the trabeculae.[14] Confocal microscopy has been used to detect intracellular $Ca^{2+}$ mainly under resting conditions in isolated myocytes[39] or trabeculae and after the cardiac arrest in whole hearts.[40]

## Funding

This work was supported by a Grant-in-Aid for Scientific Research (C) from Japan Society for the Promotion of Science (M. Miura, No. 20590205).

## Disclosures

None of the authors report conflicts of interest.

## References


1. Chen PS, Joung B, Shinohara T, Das M, Chen Z, Lin SF. The initiation of the heart beat. *Circ J* 2010; **74:** 221–225.
2. Janse MJ. Electrophysiological changes in heart failure and their relationship to arrhythmogenesis. *Cardiovasc Res* 2004; **61:** 208–217.
3. Myerburg RJ, Interian A, Mitrani RM, Kessler KM, Castellanos A. Frequency of sudden cardiac death and profiles of risk. *Am J Cardiol* 1997; **80:** 10F–19F.
4. Pogwizd SM. Nonreentrant mechanisms underlying spontaneous ventricular arrhythmias in a model of nonischemic heart failure in rabbits. *Circulation* 1995; **92:** 1034–1048.
5. Priori SG, Mantica M, Schwartz PJ. Delayed afterdepolarizations elicited in vivo by left stellate ganglion stimulation. *Circulation* 1988; **78:** 178–185.
6. Verkerk AO, Veldkamp MW, Baartscheer A, Schumacher CA, Klöpping C, van Ginneken AC, et al. Ionic mechanism of delayed afterdepolarizations in ventricular cells isolated from human end-stage failing hearts. *Circulation* 2001; **104:** 2728–2733.
7. Liu N, Rizzi N, Boveri L, Priori SG. Ryanodine receptor and calsequestrin in arrhythmogenesis: What we have learnt from genetic diseases and transgenic mice. *J Mol Cell Cardiol* 2009; **46:** 149–159.
8. Beuckelmann DJ, Näbauer M, Erdmann E. Intracellular calcium handling in isolated ventricular myocytes from patients with terminal heart failure. *Circulation* 1992; **85:** 1046–1055.
9. Eisner DA, Kashimura T, Venetucci LA, Trafford AW. From the ryanodine receptor to cardiac arrhythmias. *Circ J* 2009; **73:** 1561–1567.
10. ter Keurs HE, Boyden PA. Calcium and arrhythmogenesis. *Physiol Rev* 2007; **87:** 457–506.
11. Young AA, Dokos S, Powell KA, Sturm B, McCulloch AD, Starling RC, et al. Regional heterogeneity of function in nonischemic dilated cardiomyopathy. *Cardiovasc Res* 2001; **49:** 308–318.
12. Siogas K, Pappas S, Graekas G, Goudevenos J, Liapi G, Sideris DA. Segmental wall motion abnormalities alter vulnerability to ventricular ectopic beats associated with acute increases in aortic pressure in patients with underlying coronary artery disease. *Heart* 1998; **79:** 268–273.
13. Miura M, Nishio T, Hattori T, Murai N, Stuyvers BD, Shindoh C, et al. Effect of nonuniform muscle contraction on sustainability and frequency of triggered arrhythmias in rat cardiac muscle. *Circulation* 2010; **121:** 2711–2717.
14. Wakayama Y, Miura M, Stuyvers BD, Boyden PA, ter Keurs HE. Spatial nonuniformity of excitation-contraction coupling causes arrhythmogenic $Ca^{2+}$ waves in rat cardiac muscle. *Circ Res* 2005; **96:** 1266–1273.
15. Miura M, Boyden PA, ter Keurs HEDJ. $Ca^{2+}$ waves during triggered propagated contractions in intact trabeculae: Determinants of the velocity of propagation. *Circ Res* 1999; **84:** 1459–1468.
16. Sugai Y, Miura M, Hirose M, Wakayama Y, Endoh H, Nishio T, et al. Contribution of $Na^+/Ca^{2+}$ exchange current to the formation of delayed afterdepolarizations in intact rat ventricular muscle. *J Cardiovasc Pharmacol* 2009; **53:** 517–522.
17. Fedida D, Noble D, Rankin AC, Spindler AJ. The arrhythmogenic transient inward current iTI and related contraction in isolated guinea-pig ventricular myocytes. *J Physiol* 1987; **392:** 523–542.
18. Dash R, Frank KF, Carr AN, Moravec CS, Kranias EG. Gender influences on sarcoplasmic reticulum $Ca^{2+}$-handling in failing human myocardium. *J Mol Cell Cardiol* 2001; **33:** 1345–1353.
19. Sipido KR, Volders PG, Vos MA, Verdonck F. Altered Na/Ca exchange activity in cardiac hypertrophy and heart failure: A new target for therapy? *Cardiovasc Res* 2002; **53:** 782–805.
20. Cheng H, Lederer WJ. Calcium sparks. *Physiol Rev* 2008; **88:** 1491–1545.
21. Bers DM, Eisner DA, Valdivia HH. Sarcoplasmic reticulum $Ca^{2+}$ and heart failure: Roles of diastolic leak and $Ca^{2+}$ transport. *Circ Res* 2003; **93:** 487–490.
22. Song LS, Pi Y, Kim SJ, Yatani A, Guatimosim S, Kudej RK, et al. Paradoxical cellular $Ca^{2+}$ signaling in severe but compensated canine left ventricular hypertrophy. *Circ Res* 2005; **97:** 457–464.
23. Shorofsky SR, Aggarwal R, Corretti M, Baffa JM, Strum JM, Al-Seikhan BA, et al. Cellular mechanisms of altered contractility in the hypertrophied heart: Big hearts, big sparks. *Circ Res* 1999; **84:** 424–434.
24. Gómez AM, Valdivia HH, Cheng H, Lederer MR, Santana LF, Cannell MB, et al. Defective excitation-contraction coupling in experimental cardiac hypertrophy and heart failure. *Science* 1997; **276:** 800–806.
25. Endo H, Miura M, Hirose M, Takahashi J, Nakano M, Wakayama Y, et al. Reduced inotropic effect of nifekalant in failing hearts in rats. *J Pharmacol Exp Ther* 2006; **318:** 1102–1107.
26. Handoko ML, Schalij I, Kramer K, Sebkhi A, Postmus PE, van der Laarse WJ, et al. A refined radio-telemetry technique to monitor right ventricle or pulmonary artery pressures in rats: A useful tool in pulmonary hypertension research. *Pflugers Arch* 2008; **455:** 951–959.
27. Lamberts RR, Hamdani N, Soekhoe TW, Boontje NM, Zaremba R, Walker LA, et al. Frequency-dependent myofilament $Ca^{2+}$ desensitization in failing rat myocardium. *J Physiol* 2007; **582:** 695–709.
28. Kögler H, Hartmann O, Leineweber K, Nguyen van P, Schott P, Brodde OE, et al. Mechanical load-dependent regulation of gene expression in monocrotaline-induced right ventricular hypertrophy in the rat. *Circ Res* 2003; **93:** 230–237.
29. Engelhardt S, Hein L, Dyachenkow V, Kranias EG, Isenberg G, Lohse MJ. Altered calcium handling is critically involved in the cardiotoxic effects of chronic beta-adrenergic stimulation. *Circulation* 2004; **109:** 1154–1160.
30. Housmans PR, Lee NKM, Blinks JR. Active shortening retards the decline of the intracellular calcium transient in mammalian heart muscle. *Science* 1983; **221:** 159–161.
31. Daniels MCG, ter Keurs HEDJ. Spontaneous contractions in rat cardiac trabeculae: Trigger mechanism and propagation velocity. *J Gen Physiol* 1990; **95:** 1123–1137.
32. Schmidt U, Hajjar RJ, Helm PA, Kim CS, Doye AA, Gwathmey JK. Contribution of abnormal sarcoplasmic reticulum ATPase activity to systolic and diastolic dysfunction in human heart failure. *J Mol Cell Cardiol* 1998; **30:** 1929–1937.
33. Bers DM. Cardiac excitation-contraction coupling. *Nature* 2002; **415:** 198–205.
34. Ching LL, Williams AJ, Sitsapesan R. Evidence for $Ca^{2+}$ activation and inactivation sites on the luminal side of the cardiac ryanodine receptor complex. *Circ Res* 2000; **87:** 201–206.
35. Meissner G, Rios E, Tripathy A, Pasek DA. Regulation of skeletal muscle $Ca^{2+}$ release channel (ryanodine receptor) by $Ca^{2+}$ and monovalent cations and anions. *J Biol Chem* 1997; **272:** 1628–1638.
36. Rousseau E, Meissner G. Single cardiac sarcoplasmic reticulum $Ca^{2+}$-release channel: Activation by caffeine. *Am J Physiol* 1989; **256:** H328–H333.
37. Marks AR. Cardiac intracellular calcium release channels: Role in heart failure. *Circ Res* 2000; **87:** 8–11.
38. Jiang D, Xiao B, Yang D, Wang R, Choi P, Zhang L, et al. RyR2 mutations linked to ventricular tachycardia and sudden death reduce the threshold for store-overload-induced $Ca^{2+}$ release (SOICR). *Proc Natl Acad Sci USA* 2004; **101:** 13062–13067.
39. Cheng H, Lederer WJ, Cannell MB. Calcium sparks: Elementary events underlying excitation-contraction coupling in heart muscle. *Science* 1993; **262:** 740–744.
40. Fujiwara K, Tanaka H, Mani H, Nakagami T, Takamatsu T. Burst emergence of intracellular $Ca^{2+}$ waves evokes arrhythmogenic oscillatory depolarization via the $Na^+$-$Ca^{2+}$ exchanger: Simultaneous confocal recording of membrane potential and intracellular $Ca^{2+}$ in the heart. *Circ Res* 2008; **103:** 509–518.


## Supplemental Files

**Supplemental File 1**

**Data S1.** Methods

Please find supplemental file(s);
http://dx.doi.org/10.1253/circj.CJ-10-1050